Experimental Simulation of Neutron Irradiation Effects on Stainless Steel 304H Using Non-Irradiation Method

Hyeonje Ryoo [a], Junhyuk Ham [a], Ji Hyun Kim [a*]

Department of Nuclear Engineering, College of Engineering, Ulsan National Institute of Science and Technology 50, UNIST-gil, Ulsan 44919, Republic of Korea

[*]Corresponding author: kimjh@unist.ac.kr

***Keywords :** 304H stainless steel, Sensitization heat treatment, Warm rolling, STEM, SEM*

1. Introduction

The reactor environment includes extreme conditions such as high temperature, high pressure, and radiation exposure. Ensuring the reliability and predicting the lifespan of structural materials in such an environment is a critical research topic in the nuclear industry. Stainless steel 304H, a type of austenitic stainless steel, is widely used as a structural material in nuclear power plants due to its excellent corrosion resistance, provided by the chromium oxide layer, and its high mechanical properties at elevated temperatures. However, neutron irradiation induces defects within the material, leading to changes in both mechanical and microstructural properties. Therefore, evaluating the integrity of neutron-irradiated structural materials is of utmost importance.

According to previous studies, radiation exposure generates vacancies and interstitials, which lead to radiation-induced segregation (RIS), particularly at grain boundaries where diffusion coefficients are high. This phenomenon results in the depletion and enrichment of specific elements at the grain boundary, leading to chromium depletion and consequently reducing corrosion resistance. Additionally, defects generated by neutron irradiation cause stress concentration within the material. The combination of these effects increases the susceptibility to intergranular stress corrosion cracking (IGSCC), which has been observed in actual reactor components, such as baffle former bolts, where SCC has occurred. Therefore, assessing the impact of neutron irradiation is crucial for ensuring the integrity of nuclear power plants. However, direct evaluation of neutron-irradiated materials is highly dangerous and expensive, making it practically challenging.

This study aims to systematically investigate the effects of neutron irradiation and simulate the irradiation-induced phenomena in a non-irradiative manner. Sensitization heat treatment will be used to form chromium carbides, thereby mimicking chromium depletion caused by RIS. Additionally, warm rolling will be employed to induce defects while minimizing the formation of undesired martensitic phases, thereby simulating yield strength changes due to irradiation-induced defects. The microstructural changes will be examined using scanning electron microscopy (SEM) to confirm the presence of chromium carbides, while scanning transmission electron microscopy (STEM) and energy-dispersive spectroscopy (EDS) will be utilized to analyze chromium depletion at the grain boundary. Finally, tensile testing will be conducted to evaluate whether the yield strength of the warm-rolled material adequately replicates the effects of irradiation-induced defects.

2. Experimental and Results

2.1 Experimental

2.1.1 Materials

The material used in this study is stainless steel 304H. Specifically, the high-carbon content variant, denoted as the H grade, was utilized. The chemical composition is detailed in Table 1.

Table 1: Chemical composition (in wt.%) of stainless steel 304H used in this study

Fe	C	Si	Mn	P
Bal.	0.0542	0.0429	1.069	0.0158
Cr	Ni	Cu	Co	
18.25	8.055	0.027	0.022	

In previous studies, the major degradation phenomena caused by neutron irradiation were identified to simulate its effects. According to the prior research by G.W. Was, radiation-induced segregation (RIS) due to neutron irradiation reduces the corrosion resistance at grain boundaries and leads to stress concentration at the grain boundaries due to defect formation, which is considered a major cause of stress corrosion cracking (SCC). This

study explains that neutron irradiation depletes chromium at grain boundaries, and when the chromium content falls below 14 wt.%, the material exhibits an increased tendency for intergranular stress corrosion cracking (IGSCC), directly affecting corrosion behavior. Additionally, defect formation leads to material hardening and an increase in yield strength, causing stress concentration at the grain boundaries and further increasing the susceptibility to IGSCC. It is reported that IGSCC susceptibility is highest when the yield strength reaches 800 MPa, and when neutron irradiation exceeds 5 dpa, the yield strength of the material converges to 800 MPa. Based on this, the study aims to simulate the material subjected to neutron irradiation effects at 5 dpa [1].

To simulate the radiation-induced segregation (RIS) phenomenon, the chromium depletion tendency due to sensitization heat treatment was first examined. It was observed that as the sensitization temperature increased, the chromium depletion width became wider and occurred more rapidly compared to the change in chromium content. Since RIS due to neutron irradiation occurs in a very narrow region, this characteristic was considered, and the heat treatment was conducted at the lowest possible temperature. As shown in Fig. 1, the phase diagram was analyzed to determine the appropriate conditions: solution annealing was performed at 1040°C, followed by sensitization heat treatment at 700°C to prevent the formation of unwanted ferrite phases [2].

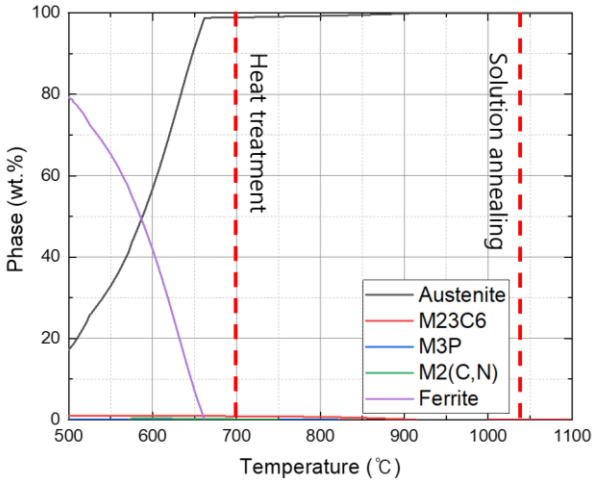

Fig. 1. Phase diagram of SS304 [3]

Additionally, to predict the extent of chromium depletion, previous studies were reviewed to determine the chromium depletion levels under different sensitization heat treatment conditions. The formation of chromium carbides was analyzed based on chemical composition, temperature, and time using TTT diagrams generated by JMatPro. This approach allowed for the estimation of chromium depletion over time in stainless steel 304H.

Table 2: In prior research papers, the trend of Cr changes in SS304 was compared with the calculation results of M23C6 using JmatPro [2, 3, 4, 5, 6]

Author	Temp. (℃)	Time (h)	$M_{23}C_6$ (at.%) [3]	△Cr (wt.%)
Bruemmer [4]	600	9	0.0298	5.38
	600	57	0.2266	6.58
	600	100	0.3986	7.08
	625	25	0.17	7.28
Butler [2]	600	2	0.00645	3.8
	600	2	0.00645	1.9
	675	2	0.0401	6.5
	675	2	0.0401	6
	675	2	0.0401	5.5
	675	2	0.0401	4.9
Bruemmer	700	1	0.0226	5.98
	700	10	0.3	7.08
	700	100	1.25	6.58
Ravindra [5]	700	2	0.0436	6.011
	700	24	0.55	8.711
	700	96	0.89	8.011
Trillo [6]	775	10	0.52	4.79
Bruemmer	800	10	0.85	3.88

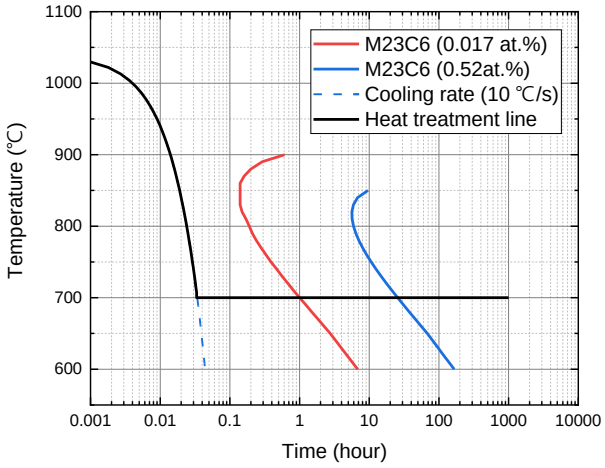

Fig. 2. TTT diagram for $M_{23}C_6$ of SS 304H [3]

Through this analysis, sensitization heat treatment conditions ranging from 1 hour to 12 hours were determined. The final sensitization heat treatment conditions are presented in Table III.

Table 3: The sensitization heat treatment conditions

Annealing temperature [℃]	1040
Annealing time	2 h
Sensitization temperature [℃]	700
Sensitization time [h]	1, 2, 3, 5, 7, 15, 24
Cooling	Water quenched

After sensitization heat treatment, warm rolling was conducted to simulate the mechanical strengthening effect of irradiation hardening. During the rolling process, an increase in rolling temperature suppresses the formation of the martensite phase. To minimize the formation of unwanted martensite, warm rolling was performed at 200°C. The required reduction ratio to achieve the target yield strength of 800 MPa through cold rolling was identified from previous studies, indicating that a reduction of 20–25% would be sufficient to reach the target yield strength. However, since warm rolling was employed in this study, a higher reduction ratio was necessary. Therefore, warm rolling was performed with a maximum reduction of 30% [7, 8].

2.1.2. Microstructure analysis

All materials were examined for their microstructure using Scanning Electron Microscopy (SEM), while materials subjected to heat treatment were assessed for the formation of Cr carbides. Furthermore, to investigate the chromium-depleted regions around Cr carbides, Transmission Electron Microscopy (TEM) samples were fabricated using Focused Ion Beam (FIB). Scanning Transmission Electron Microscopy (STEM) coupled with Energy Dispersive X-ray Spectroscopy (EDS) was employed to quantify the extent and

chromium depletion in the surrounding areas. This data was then compared with neutron-irradiated materials.

2.1.3. Mechanical properties analysis

Tensile specimens were fabricated in accordance with ASTM E8M dimensions, as illustrated in Fig. 3 To minimize variations in mechanical properties induced by the rolling direction, specimens were prepared in the Transverse Direction (TD) from the Rolling Direction (RD), as depicted in Fig. 4 Tensile tests were conducted at room temperature, and the testing was carried out at a rate of 0.015 mm/mm/min [9].

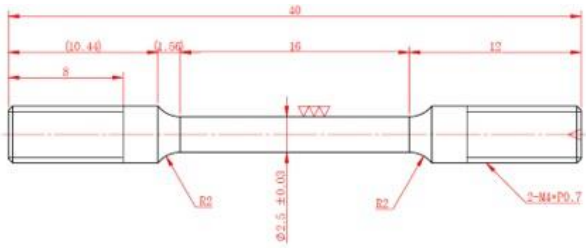

Fig. 3. Tensile specimens

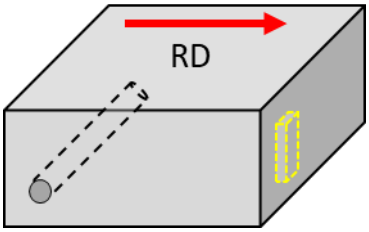

Fig. 4. Rolling direction and specimen direction

2.2. Results

2.2.1. Microstructure and hardness

First, the grain size and hardness of the material were measured. The results showed that grain size and hardness were not significantly affected by sensitization heat treatment. However, grain size decreased considerably due to rolling, and the changes in grain size according to the reduction rate are presented in Fig. 5. Additionally, optical microscopy results in Fig. 6 confirmed the suppression of the martensitic phase due to rolling, with little to no formation observed.

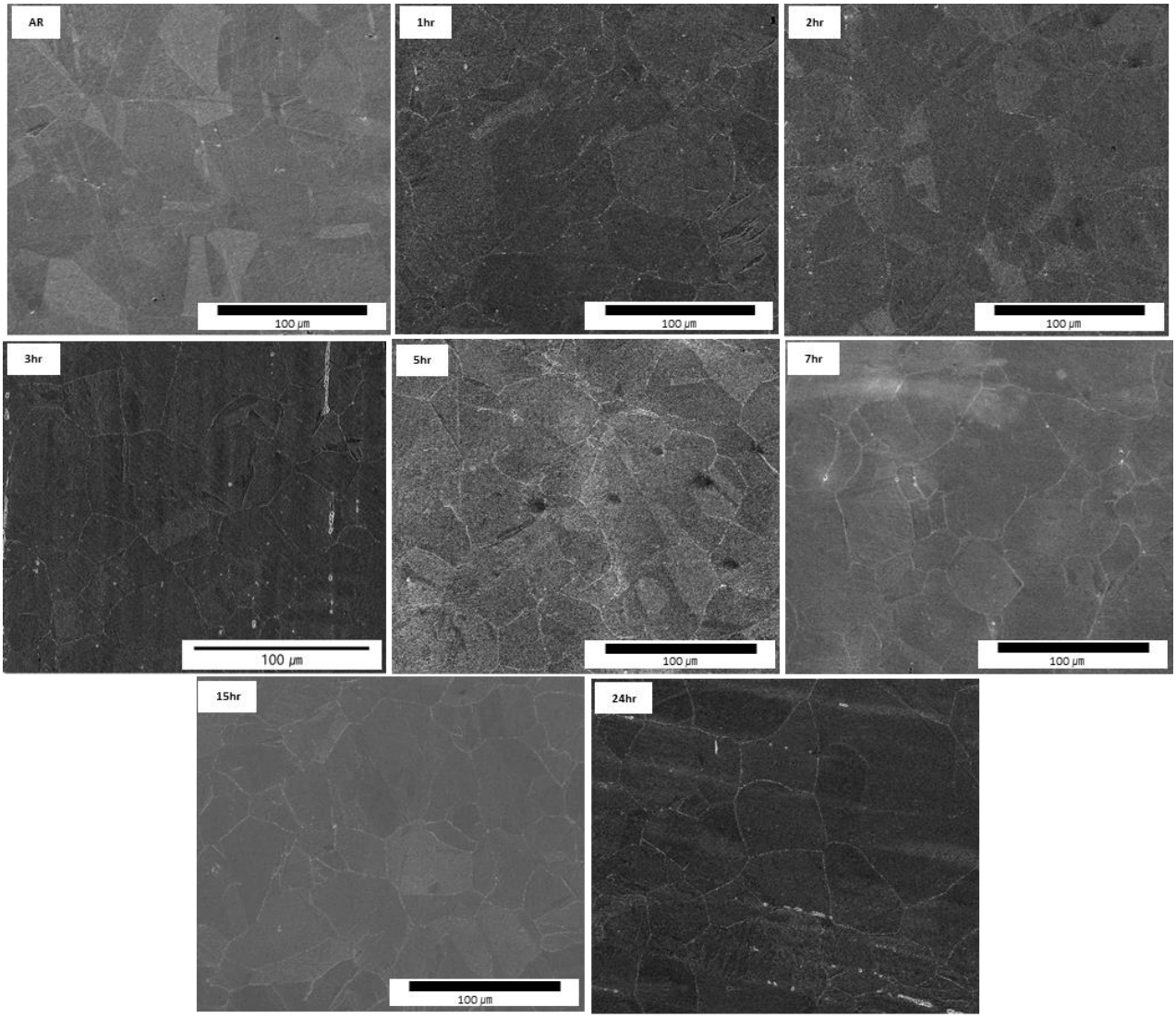

Fig. 5. Low-magnification SEM image

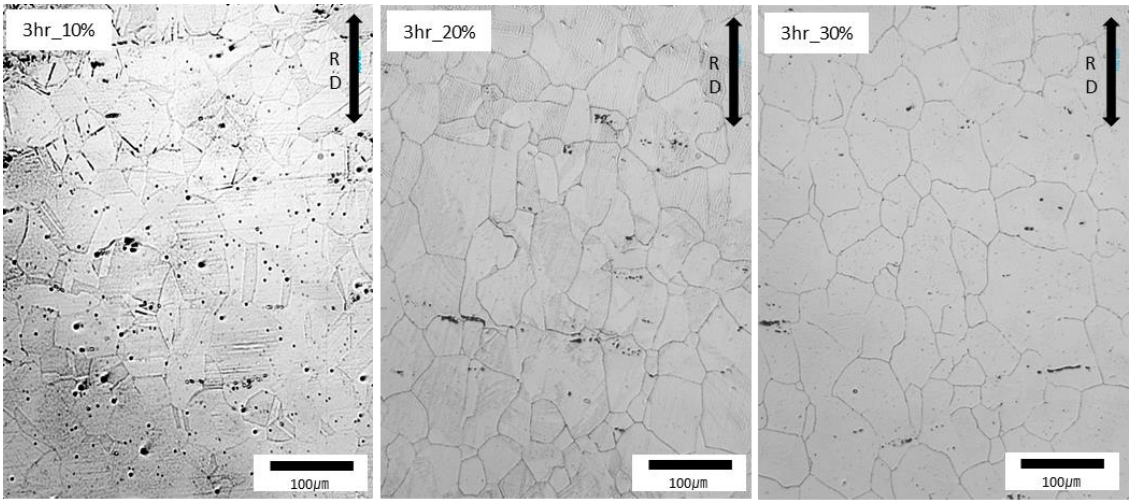

Fig. 6. Rolled material OM image

Table 4: Grain size and hardness according to conditions

Sensitization time (hr)	**AR**	**1**	**2**	**3**				**5**	**7**	**15**	**24**
Reduction rate (%)	**0**	**0**	**0**	**0**	**10**	**20**	**30**	**0**	**0**	**0**	**0**
Grain Size (㎛)	51.02	48.11	48.52	48.11	36.21	30.89	27.83	48.80	43.73	42.63	44.31
Hardness (HV)	171.7	168.2	161.3	162.2	233.2	271.4	285.6	161.2	154.4	172.4	176.1

Additionally, the formation of chromium carbides due to sensitization heat treatment is shown in Fig. 7. Since carbide formation leads to localized chromium depletion, the amount of carbide formation was analyzed as a function of sensitization time. Most carbides were found to form along grain boundaries, and as carbide formation increased, the surrounding chromium content was expected to decrease further.

To verify this, high-magnification SEM images in Fig. 8 were used to measure the carbide formation area along the grain boundary length. This analysis allowed for the evaluation of chromium carbide density variations with sensitization time. The results showed that as sensitization time increased, carbide density also increased. However, over time, the rate of increase in carbide density gradually slowed.

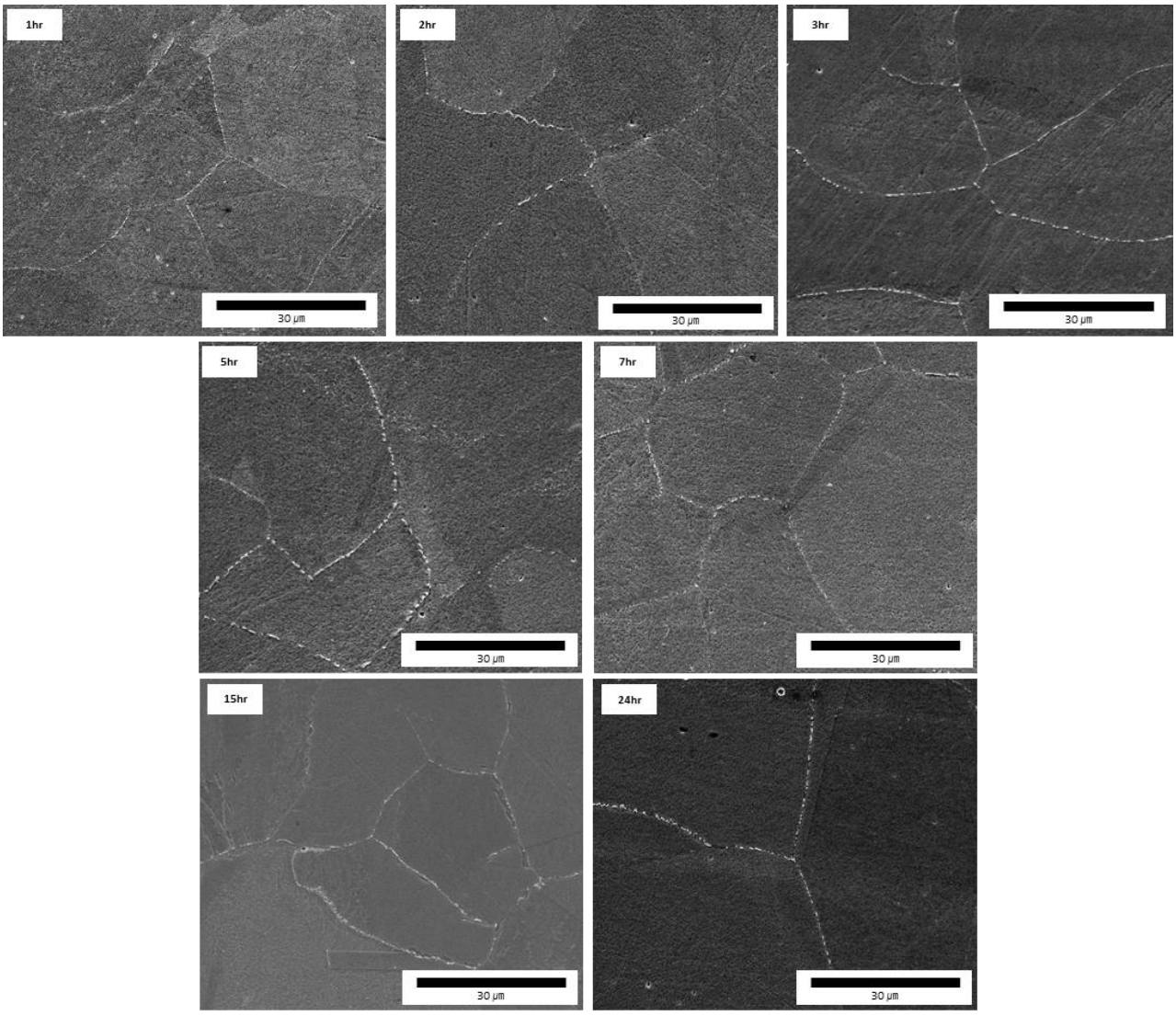

Fig. 7. High-magnification SEM image

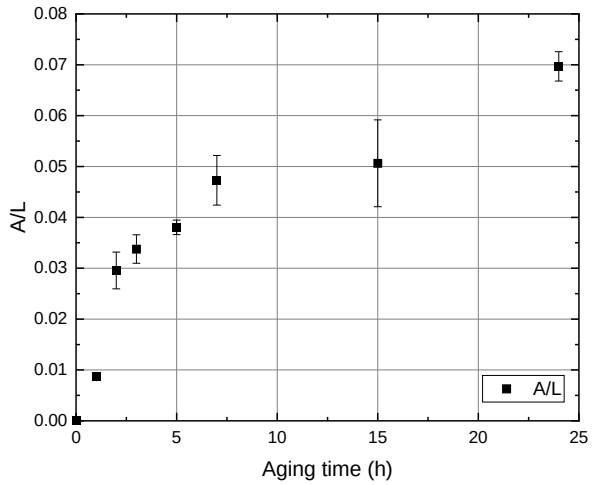

Fig. 8. Cr Carbide Density as a Function of Sensitization Time

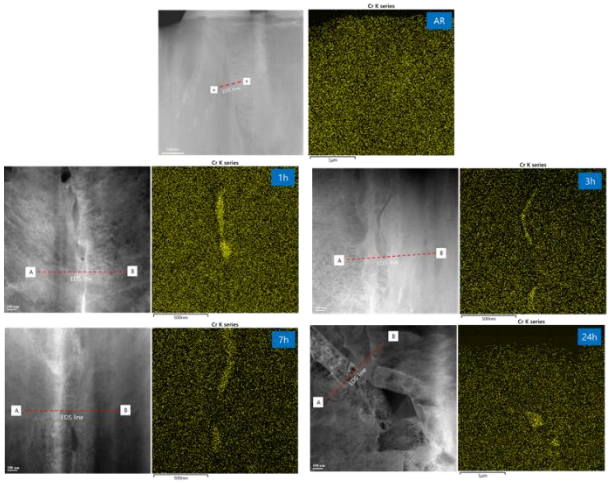

Fig. 9. STEM Image and EDS Map of Sensitization Time

2.2.2. Evaluation of simulation accuracy in Cr depletion

Since accurately determining chromium content at the SEM level is challenging, STEM-EDS analysis was conducted to precisely evaluate the chromium depletion trend as a function of sensitization time. Chromium content near grain boundaries surrounding chromium carbides was analyzed using STEM-EDS.

Fig. 9 presents the EDS chromium map and data acquisition images obtained via EDS line scans. The chromium carbides were identified through the Cr mapping results. To minimize the effects of diffusion, chemical composition was measured at grain boundaries located 100–150 nm away from the carbides. The results of the EDS line scans are shown in Fig. 10.

Table V summarizes the width and magnitude of chromium depletion as a function of sensitization time. The results indicate that during the initial stages of sensitization, chromium depletion occurs rapidly, but after 3 hours, the rate of change in chromium content stabilizes, while the depletion width continues to expand significantly. Between 7 and 24 hours, the minimum chromium content remains nearly unchanged, with only the depletion width increasing.

Additionally, the chromium depletion due to neutron irradiation at the target level of 5 dpa was approximately 5 wt.%. In comparison, 3 hours of sensitization heat treatment resulted in a chromium depletion of approximately 6 wt.%, making it the most suitable condition for simulating irradiation-induced chromium depletion.

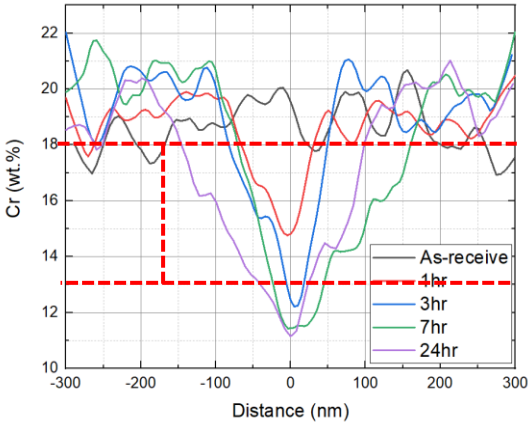

Fig. 10. Cr Depletion in sensitization Material Observed by EDS

Table 5: EDS results of sensitized heat-treated material

Heat treatment time (Hour)	Min. of Cr (wt.%)	Depletion width (nm)
1	14.8	150
3	12.2	180
7	11.4	250
24	11.1	300

Subsequently, STEM-EDS analysis was conducted on the warm-rolled material under the same conditions to evaluate chromium depletion. The results showed that chromium depletion remained nearly unchanged.

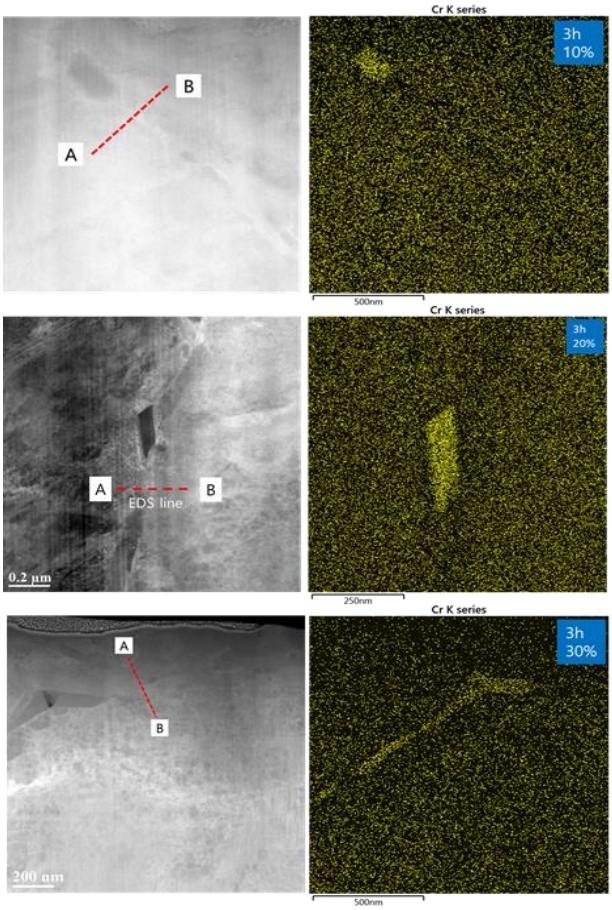

Fig. 11. STEM Image and EDS Map of Rolled Material

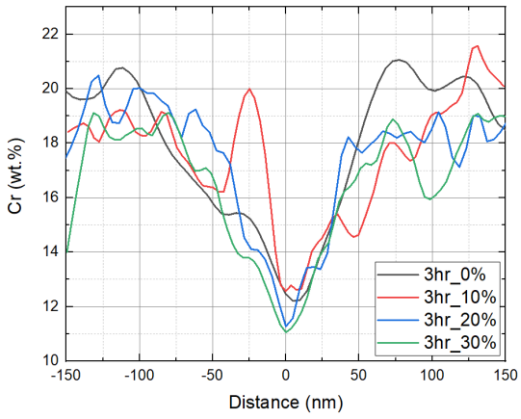

Fig. 12. Cr Depletion in Rolled Material Observed by EDS

2.2.3. Evaluation of simulation accuracy in Mechanical properties

The results of the tensile test conducted to evaluate the mechanical strength of the warm-rolled material are presented in Fig. 13. Yield strength, ultimate tensile strength, and elongation were measured, with detailed values summarized in Table VI. As the reduction rate increased, both yield strength and ultimate tensile strength showed an increasing trend. Notably, the yield strength reached 793 MPa at a 30% reduction rate. Conversely, elongation decreased with an increasing reduction rate.

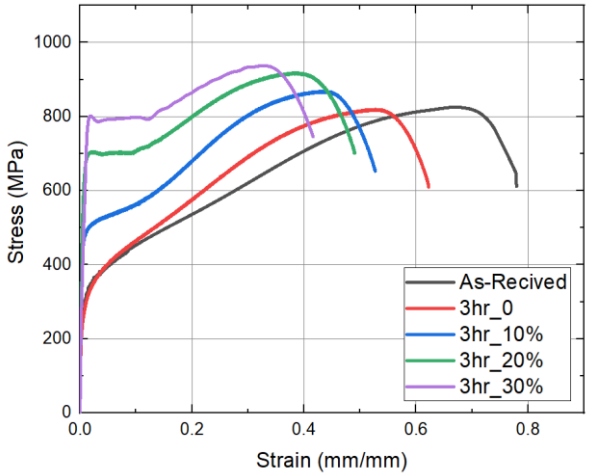

Fig. 13. Tensile test strain-stress curve

Table 6: Tensile test results

Reduction rate	AR	3hr, 0%	3hr, 10%	3hr, 20%	3hr, 30%
YS (MPa)	300	321	520	687	793
Dev	7.5	8.3	12.5	15.0	2.7
UTS (MPa)	820	819	833	913	937
Elongation	0.78	0.62	0.53	0.49	0.42

Additionally, the yield strength of the simulated material was calculated using Equation 1, based on previous studies comparing the hardness and yield strength of neutron-irradiated materials. The experimentally measured yield strength was then compared with the yield strength converted from hardness values, as shown in Fig. 14.

Fig. 14 confirms that the calculated yield strength closely matches the experimentally obtained values. It was observed that the hardening effect caused by neutron irradiation and the grain refinement-induced hardening due to warm rolling resulted in similar yield strength values. However, when the irradiation dose was high and the hardness increased by more than 100 Hv, slight discrepancies were observed due to irradiation-induced unique defects. At lower irradiation doses, irradiation hardening exhibited a mechanical strength trend similar to that induced by rolling [10].

$$\Delta\sigma = 3.63\Delta H_v (H_v < 100, dose < 3dpa)$$
$$\Delta\sigma = 2.13\Delta H_v (H_v > 100, dose > 3dpa)$$

Eq. 1. Conversion formula between yield strength and hardness values for neutron-irradiated materials [10]

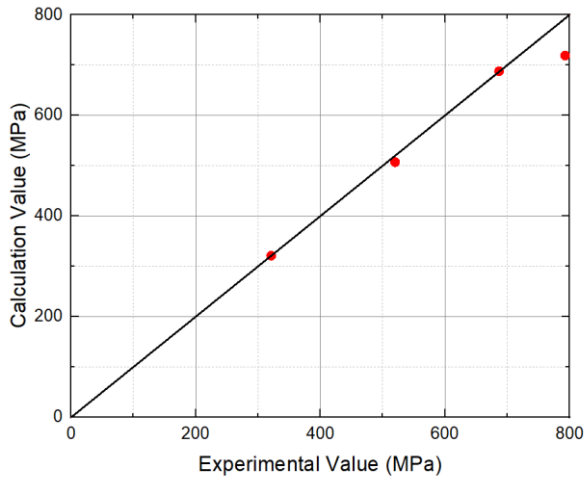

Fig. 14. Comparison Graph of Yield Strength Obtained by Converting the Measured Yield Strength and Hardness Values in This Study

3. Conclusions

This study aimed to simulate the effects of neutron irradiation on stainless steel 304H by inducing chromium depletion and mechanical property changes through sensitization heat treatment and warm rolling. Sensitization heat treatment at 700°C resulted in localized chromium depletion. STEM-EDS analysis confirmed that 3 hours of sensitization successfully replicated the radiation-induced segregation (RIS) observed at 5 dpa, with chromium depletion reaching approximately 5 wt.%, closely matching the levels found in neutron-irradiated materials. Additionally, warm rolling at 200°C effectively increased yield strength while minimizing martensitic transformation, achieving a maximum yield strength of 793 MPa at a 30% reduction rate. A comparison between the experimentally measured yield strength and the calculated values demonstrated that rolling-induced strengthening successfully replicated the hardening effects of neutron irradiation. The proposed non-irradiative simulation method presents a practical alternative for evaluating neutron irradiation-induced material degradation and offers valuable insights into the long-term integrity of reactor components. Furthermore, future SCC experiments will be conducted to investigate the susceptibility to intergranular stress corrosion cracking (IGSCC) and to verify the effectiveness of this method in simulating actual neutron irradiation degradation phenomena.

4. Acknowledgments

This research was supported by the ‘Human Resources Program in Energy Technology’ of the Korea Institute of Energy Technology Evaluation and Planning(KETEP), which was funded by the Ministry of Trade, Industry & Energy(MOTIE. Korea). (No. RS-2024-00398425)

REFERENCES

[1] G. S. Was et al., Fundamentals of Radiation Materials Science, 2017

[2] E. P. Butler et al., CHROMIUM DEPLETION AND MARTENSITE FORMATION AT GRAIN BOUNDARIES IN SENSITISED AUSTENITIC STAINLESS STEEL, Acta Metallurgica, 1985

[3] JmatPro v11.2

[4] S. M. Bruemmer and L. A. Charlot et al., Scripta METALLURGICA (1986)

[5] Ravindra V. Taiwade et al., ISIJ International Vol. 52 (2012)

[6] E.A. Trillo, R. Beltran et al. Materials Characterization (1995)

[7] G. B. Olson et al., Kinetics of Strain-Induced Martensitic Nucleation, Metallurgical Transactions A, 1975

[8] M. Milad et al., Journal of Materials Processing Technology (2008)

[9] ASTM E8M, Standard Test Methods for Tension Testing of Metallic Materials, 2022

[10] Jeremy T. Busby et al., Journal of Nuclear Materials (2005)